Hybrid Modeling and Control of a Buck-Boost Converter with Parallel-Series Inductor Dynamics

Sergio Rojas-Yanten, Hector Espinoza-Roman

https://doi.org/10.1590/SciELOPreprints.15945

Submitted on: 2026-04-24
Posted on: 2026-05-12 (version 1)
(YYYY-MM-DD)

Hybrid Modeling and Control of a Buck-Boost Converter with Parallel-Series Inductor Dynamics

Sergio Rojas-Yantén
Facultad de Ciencias de la Ingeniería
Fundación Universitaria Antonio de Arévalo
Cartagena, Colombia
sergio.yanten@unitecnar.edu.co
ORCID: https://orcid.org/0009-0004-7077-413X

Hector Espinoza-Roman
Dirección de Investigación e Innovación
Fundación Universitaria Antonio de Arévalo
Cartagena, Colombia
hector.espinoza@unitecnar.edu.co
ORCID: https://orcid.org/0000-0002-2861-2442

April 24, 2026

Abstract

This paper presents the event-driven modeling and simulation of a DC/DC Buck-Boost converter that operates through parallel charging and series discharging of its inductors. Treated as a hybrid system with three physically realizable topologies, the model captures the complete switching dynamics through zero-crossing detection, overcoming the limitations of the conventional averaged model. Three control schemes are implemented and compared open-loop with pulse-width modulation (PWM), peak current mode control (PCMC), and PCMC with proportional-integral control and compensation ramp (PCMC-PI). The results, validated against specialized commercial software, demonstrate the correct operation of the converter and its model, which can be implemented in various applications where voltage amplification requires values up to 100 V. The model constitutes the basis for, as an example, a modular solar battery charging system with maximum power point tracking, which is proposed in future work.

Keywords: ODE Events, DC-DC power converter, Hybrid systems

1 Introduction

Power converters are fundamental components in modern electrical systems and are present in the vast majority of applications within the sector, from generation to end-use consumption. In this

context, power electronics play a predominant role in the 21st century in industrial, commercial, and residential applications, with a particular emphasis on energy efficiency and the reduction of environmental impact. [1]. This projection is supported by current trends in the global market, where the DC/DC converter segment reached USD 10.79 billion in 2023 and is projected to exceed USD 22.37 billion by 2030, driven by the increasing integration of renewable energy sources and the electrification of transport. [2]. The scale of this growth is further evidenced by the fact that, in 2023 alone, 191 GW of photovoltaic capacity were added globally, all of which require power conversion stages for integration into the electrical grid. [3]. In this scenario, it is expected that, in the future, the majority of the electrical energy delivered to the end user will pass through some form of power conversion device. [4].

Within the broad taxonomy of power converters, DC/DC devices occupy a central role in the integration of renewable energy sources, battery storage systems, and electric traction. The classical topologies available are Buck, Boost and Ćuk converters, among others. However, the Buck–Boost converter is particularly versatile, as, depending on the adjustment of its parameters, it can operate as either a step-down or a step-up converter without requiring any modification to the circuit structure. [4]. This characteristic makes it suitable for scenarios that involve wide variations in the source or load, such as those encountered in photovoltaic systems with maximum power point tracking, thus making its study particularly relevant.

However, carrying out the dynamic analysis of these devices presents a modeling challenge, as it is not a trivial task. For instance, the averaged model, widely employed in the literature due to its simplicity, neglects the switching dynamics and does not allow for the study of transient behavior or certain instability phenomena, such as subharmonic oscillations. [5]. Although non-linear extensions of this approach exist, they still omit dynamics that are relevant for rigorous control design. A more comprehensive alternative consists of treating the converter as a hybrid system, in which each operating topology is described by a set of ordinary differential equations whose transitions are determined by zero-crossing conditions. This approach, referred to as event-driven simulation, captures the complete time-domain response of the system and provides a more suitable framework for stability analysis and controller design.

Consequently, this work presents the modeling and event-driven simulation of a DC/DC Buck–Boost power converter, with the aim of providing a more flexible dynamic analysis tool than conventional approaches. Three operating configurations are developed and implemented. The first corresponds to open-loop operation with pulse-width modulation (PWM); the second to closed-loop operation with peak current mode control (PCMC); and the third incorporates proportional–integral control with slope compensation (PCMC-PI). The validity of the proposed model is verified by comparison with results obtained from specialized commercial software.

2 Mathematical Modelling of the Power Converter

2.1 Power converter

The converter under study has been previously presented in [6–9], with a variation to the proposed system through the insertion of diode D_0 (see Fig. 1).

Fig. 1 shows the converter schematic, which consists of 4 diodes (D_n), 3 controlled switches (S_n), 2 inductors with their internal resistances (L_n, R_n, respectively), a capacitor connected on the load side (C), a load resistance (R), and a voltage supply (V_{in}). The switches are assumed to turn on and off simultaneously. With the exception of the inductors, all remaining elements are

considered ideal — that is, parasitic resistances are neglected in order to simplify the analysis.

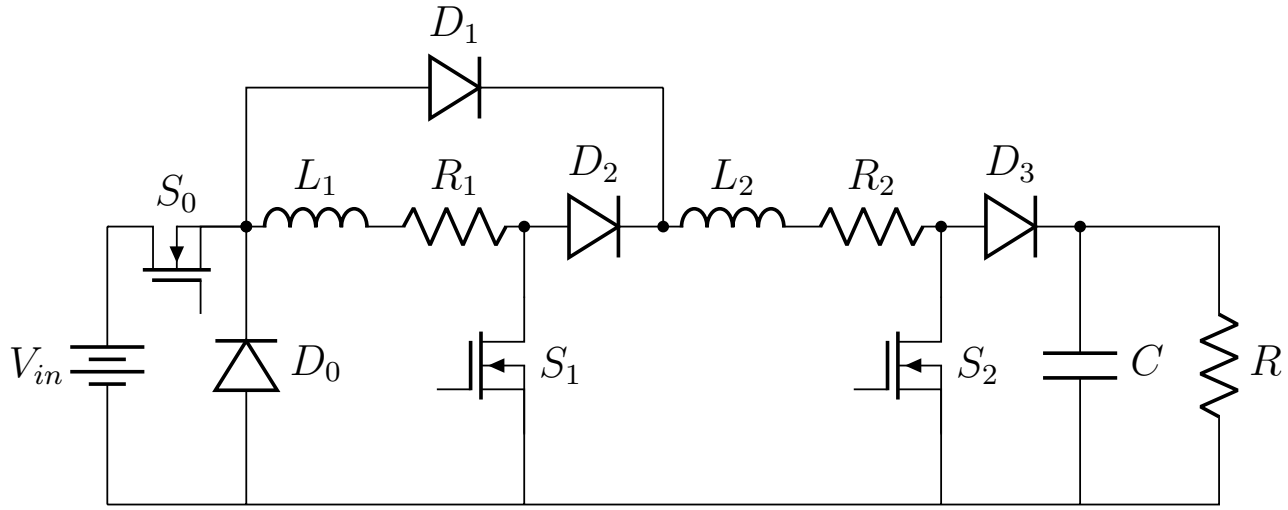

Figure 1: Buck-Boost converter proposed

Once the circuit configuration has been established, it can be observed that this device comprises seven semiconductor elements, of which four are diodes and three are controlled switches. This implies that the circuit may exhibit 128 possible operating topologies, in accordance with Equation 1 [10].

$$T_n = 2^{S_n} \tag{1}$$

Where T_n denotes the number of possible topologies and the number of semiconductor devices.

However, the circuit is subject to certain operating conditions, as the two inductors are charged in parallel using a boost-like configuration and discharged using a buck configuration. This mode of operation reduces the number of possible topologies as follows:

- The switches operate in phase; that is, they are all activated simultaneously and deactivated at the same instant. This reduces the number of possible topologies from 128 to 32.
- The biasing of diode D_0, is opposite to the conduction states of the switches, except when the converter enters discontinuous conduction mode. In other words, while D_0 is conducting, the controlled switches are non-conducting, and vice versa. This condition reduces the number of possible topologies to 17.

Taking into account the conditions outlined above, Table 1 presents the possible combinations of the converter topologies. It should be noted that the final topology corresponds to the discontinuous conduction mode (T_{17}).

Following an analysis of the topologies presented, only the combinations T_4, T_{13}, T_7 are physically feasible. These are subsequently redefined as T_1, T_2, and T_3 respectively, and are described as follows.

Table 1: Possible Combinations of Topologies

T_n	S_n	D_0	D_1	D_2	D_3
T_1	ON	OFF	ON	ON	ON
T_2	ON	OFF	ON	ON	OFF
T_3	ON	OFF	ON	OFF	ON
T_4	ON	OFF	ON	OFF	OFF
T_5	ON	OFF	OFF	ON	ON
T_6	ON	OFF	OFF	ON	OFF
T_7	ON	OFF	OFF	OFF	ON
T_8	ON	OFF	OFF	OFF	OFF
T_9	OFF	ON	ON	ON	ON
T_{10}	OFF	ON	ON	ON	OFF
T_{11}	OFF	ON	ON	OFF	ON
T_{12}	OFF	ON	ON	OFF	OFF
T_{13}	OFF	ON	OFF	ON	ON
T_{14}	OFF	ON	OFF	ON	OFF
T_{15}	OFF	ON	OFF	OFF	ON
T_{16}	OFF	ON	OFF	OFF	OFF
T_{17}	OFF	OFF	OFF	OFF	OFF

2.2 Topologies

2.2.1 Topology 1

T_1 (see Fig. 2) This corresponds to the topology in which the inductors are charged in parallel. In this topology, the diodes D_0, D_2 and D_3 are non-conducting, while the remaining semiconductor devices conduct as the control signal is in the ON state. This occurs while the capacitor discharges through the load resistance.

2.2.2 Topology 2

T_2 (see Fig. 3) This corresponds to the series discharging of the inductors in continuous conduction mode (CCM), while the capacitor connected to the load side is being charged. The controlled switches S_n and diode D_1 are non-conducting, whereas the remaining elements are conducting. In this case, the control signal is in the OFF state.

2.2.3 Topology 3

T_3 (see Fig. 4) This corresponds to the complete discharge of the inductors, entering discontinuous conduction mode (DCM). This is equivalent to an RC circuit on the load side, with a reduction in the electrical charge stored in the capacitor. In T_3, all semiconductor elements are non-conducting; additionally, the control signal is in the OFF state.

2.3 Mathematical Modelling

The system is represented in state variables by considering $x = \begin{bmatrix} v_C & i_{L_1} \end{bmatrix}^T$, where i_{L_1} and i_{L_2} are redundant elements ($i_{L_1} = i_{L_2}$) corresponding to the current flowing through the inductors, and

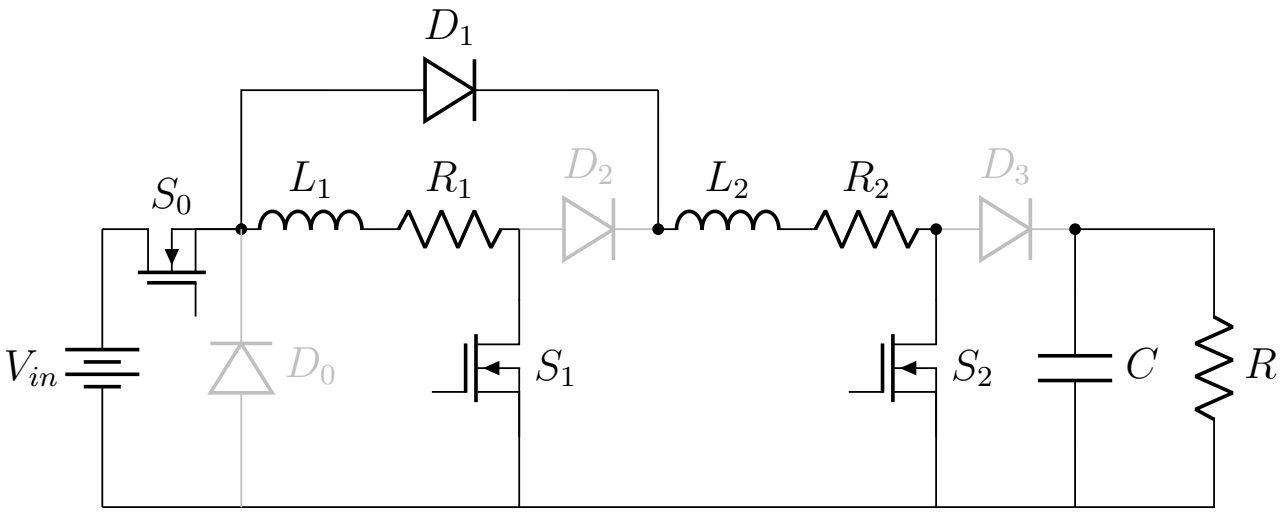

Figure 2: Topology 1, parallel inductors charging mode

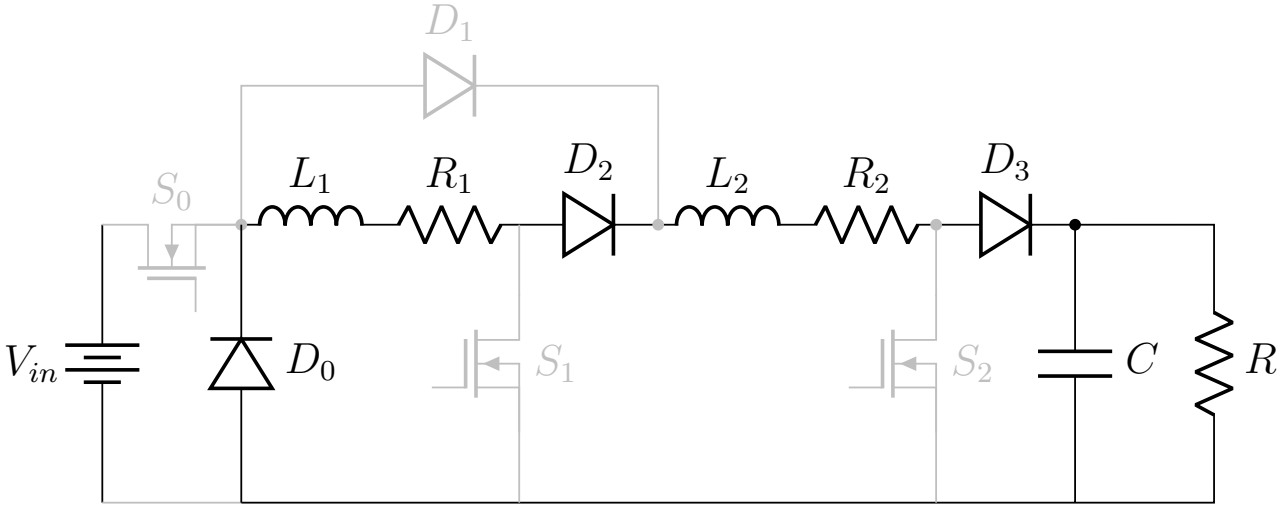

Figure 3: Topology 2, continuous conduction mode

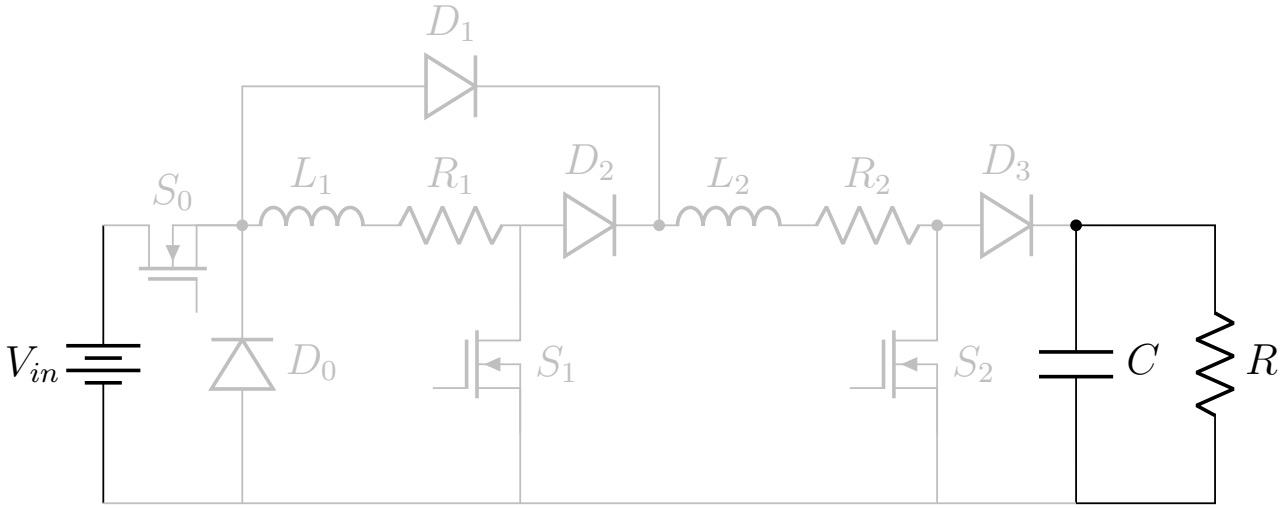

Figure 4: Topology 3, discontinuous conduction mode

v_C is the voltage across the capacitor terminals. $L_1 = L_2$, $R_1 = R_2$ y $V_D = 0$.The mathematical model of the proposed converter is presented below (Tabla 2).

Table 2: Differential Equations of the Operating Topologies

Differential Equation	***Mode***	***u***	T_n
$\dot{x} = \begin{bmatrix} -\frac{1}{RC} & 0 \\ 0 & -\frac{R_1}{L_1} \end{bmatrix} \begin{bmatrix} x_1 \\ x_2 \end{bmatrix} + \begin{bmatrix} 0 \\ \frac{1}{L_1} \end{bmatrix} V_{in}$	Charge	1	T_1
$\dot{x} = \begin{bmatrix} -\frac{1}{RC} & \frac{1}{C} \\ -\frac{1}{2L_1} & -\frac{R_1}{L_1} \end{bmatrix} \begin{bmatrix} x_1 \\ x_2 \end{bmatrix} + \begin{bmatrix} 0 \\ 0 \end{bmatrix} V_{in}$	MCC	0	T_2
$\dot{x} = \begin{bmatrix} -\frac{1}{RC} & 0 \\ 0 & 0 \end{bmatrix} \begin{bmatrix} x_1 \\ x_2 \end{bmatrix} + \begin{bmatrix} 0 \\ 0 \end{bmatrix} V_{in}$	MCD	0	T_3

Additionally:

$$\begin{aligned} T_1 &= \left\{ x \in \mathbb{R}^2 : \dot{i_L} > 0 \right\} \\ T_2 &= \left\{ x \in \mathbb{R}^2 : \dot{i_L} < 0 \right\} \\ T_3 &= \left\{ x \in \mathbb{R}^2 : \dot{i_L} = 0 \right\} \end{aligned} \tag{2}$$

3 State Diagram and Control Strategy

As previously mentioned, the proposed converter presents three operating topologies. Therefore, it has 3 states. Fig. 5 shows the state diagram of the converter in a general form.

Where T_n corresponds to the topology number and C_n to the state transition conditions.

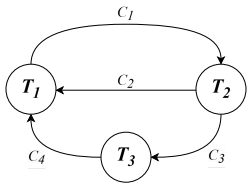

Figure 5: Open-loop state diagram.

3.1 Open loop

Fig. 6 shows the power converter controlled by a Pulse-Width Modulation (PWM) signal.

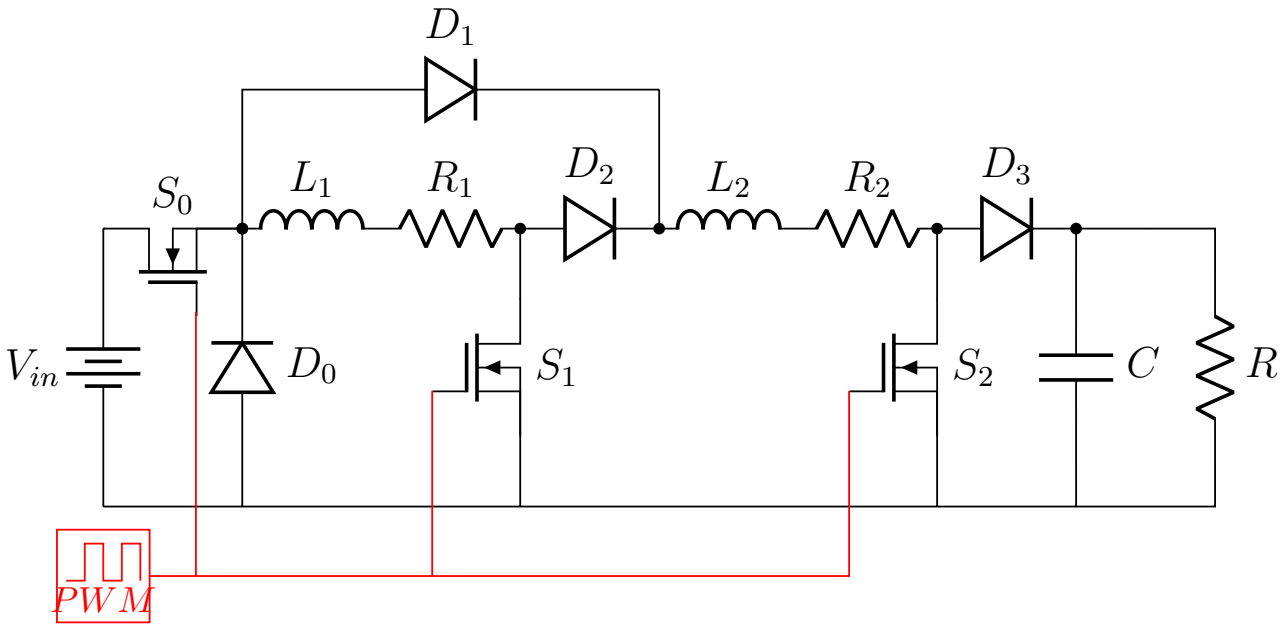

Figure 6: Proposed open-loop Buck–Boost converter

For the open loop, the following state transition conditions are considered:

$$\begin{aligned} C_1 &: t = ndT = \ mod\left(t + \frac{T}{2} - dT, T\right) - \frac{T}{2} \\ C_2 &: t = nT = \ mod\left(t - \frac{T}{2}, T\right) - \frac{T}{2} \\ C_3 &: i_L \leq 0 \\ C_4 &: t = nT = \ mod\left(t - \frac{T}{2}, T\right) - \frac{T}{2} \end{aligned} \tag{3}$$

Where d is the duty cycle, T the switching period, and n the number of each period or iteration.

3.2 Closed loop, peak current mode control (PCMC)

Peak current mode control (PCMC) is adopted as the control strategy due to the high current demand generated in the converter during transient state. To address this situation, a peak current mode control with both current and voltage loops is employed. This limits the current through the circuit, preventing the conducting elements from deteriorating or failing due to overload. Fig. 7 shows the power converter with the peak current mode control.

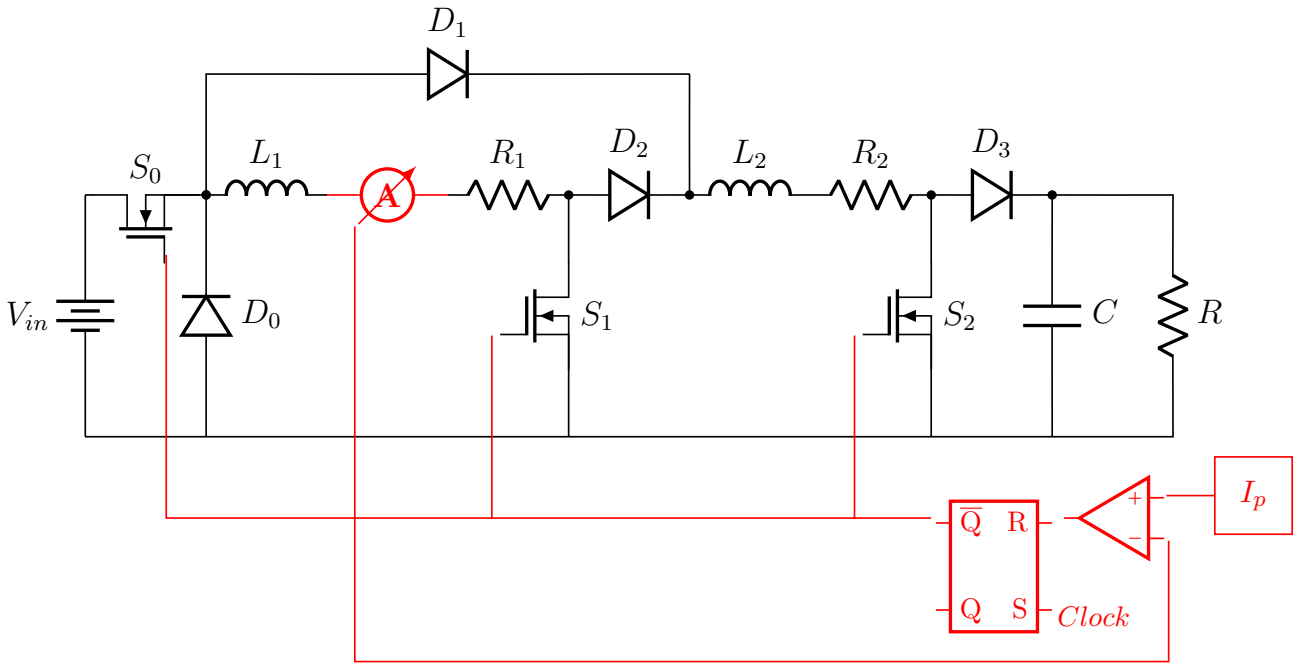

Figure 7: Buck–Boost converter with peak current mode control

The state transition conditions for peak current mode control are presented below.

$$\begin{aligned} C_1 &: I_p - i_L \leq 0 \\ C_2 &: t = nT = mod\left(t - \frac{T}{2}, T\right) - \frac{T}{2} \\ C_3 &: i_L \leq 0 \\ C_4 &: t = nT = mod\left(t - \frac{T}{2}, T\right) - \frac{T}{2} \end{aligned} \tag{4}$$

Where I_p denotes the prescribed peak current limit.

3.3 Closed-Loop Operation: Peak Current Mode Control with Proportional–Integral Regulation (PCMC-PI)

In order to introduce an additional degree of freedom and regulate the voltage, a proportional–integral (PI) controller is incorporated. Furthermore, a compensation ramp is added to increase the stability range of the system [11]. Fig. 8 illustrates the power converter with peak current mode control combined with PI regulation and a compensation ramp. Equation 5 presents the state

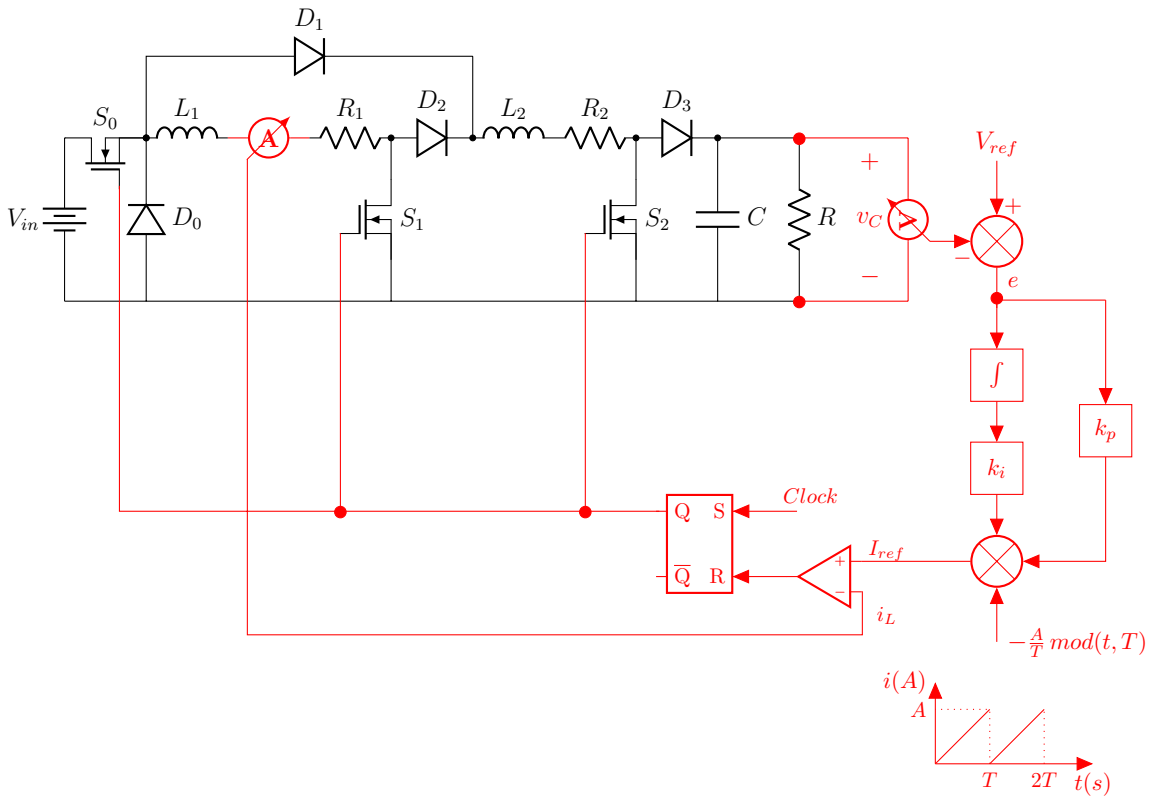

Figure 8: Buck–Boost converter with peak current mode control, PI control, and ramp compensation

transition conditions for the system under peak current mode control with proportional–integral regulation.

$$\begin{aligned} C_1 &: I_{ref} - i_L \leq 0 \\ C_2 &: t = nT = \; mod\left(t - \frac{T}{2}, T\right) - \frac{T}{2} \\ C_3 &: i_L \leq 0 \\ C_4 &: t = nT = \; mod\left(t - \frac{T}{2}, T\right) - \frac{T}{2} \end{aligned} \tag{5}$$

The control signal is denoted as I_{ref} and its calculation is found in Equation 6. Furthermore, the error signal is calculated as the difference between the reference voltage and the capacitor voltage.

$$I_{ref} = k_p\, e(t) + k_i \int e(t)\, dt - \frac{A}{T}\, mod(t, T) \tag{6}$$

Where A corresponds to the amplitude of the compensation ramp, k_p to the value of the proportional constant, and k_i is the value of the integral constant.

To include the error integral, it is necessary to redefine the equations governing the circuit. Therefore, Table 3 presents the new state space.

Table 3: Differential Equations with the New State-Space Representation

Differential Equation	***Mode***	$\boldsymbol{u}$	T_n
$\dot{x} = \begin{bmatrix} -\frac{1}{RC} & 0 & 0 \\ 0 & -\frac{R_1}{L_1} & 0 \\ -1 & 0 & 0 \end{bmatrix} \begin{bmatrix} x_1 \\ x_2 \\ x_3 \end{bmatrix} + \begin{bmatrix} 0 \\ \frac{1}{L_1} \\ \frac{V_{ref}}{V_{in}} \end{bmatrix} V_{in}$	Charge	1	T_1
$\dot{x} = \begin{bmatrix} -\frac{1}{RC} & \frac{1}{C} & 0 \\ -\frac{1}{2L_1} & -\frac{R_1}{L_1} & 0 \\ -1 & 0 & 0 \end{bmatrix} \begin{bmatrix} x_1 \\ x_2 \\ x_3 \end{bmatrix} + \begin{bmatrix} 0 \\ 0 \\ \frac{V_{ref}}{V_{in}} \end{bmatrix} V_{in}$	MCC	0	T_2
$\dot{x} = \begin{bmatrix} -\frac{1}{RC} & 0 & 0 \\ 0 & 0 & 0 \\ -1 & 0 & 0 \end{bmatrix} \begin{bmatrix} x_1 \\ x_2 \\ x_3 \end{bmatrix} + \begin{bmatrix} 0 \\ 0 \\ \frac{V_{ref}}{V_{in}} \end{bmatrix} V_{in}$	MCD	0	T_3

4 Simulations results

The modeling of power converters with differential equations and topology changes is equivalent to the simulation of non-smooth, discontinuous systems that exhibit discontinuities. This is also referred to as hybrid systems [12]. In this type of system, the exact time at which a state transition (or state event) occurs is not known while the system is evolving. However, the conditions under which a zero-crossing function can be generated in the algorithm are known. These functions depend on the state variables or on time if it is a time event, i.e., if the switching time or the time at which an event occurs is known. Furthermore, these functions must be continuously evaluated in the algorithm to detect when a condition for the zero-crossing is met and the corresponding state change is performed. To this end, the zero-crossing functions are entered into a vector for each condition of each state [13].

For the simulation, a current limit of 30 amperes is considered. Table 4 presents the simulation parameters.

The results obtained from the simulation of the converter under the configurations presented in the previous section are outlined below. These results, derived from the proposed event-driven model, are compared with those obtained using the commercial software PSIM in order to validate the findings.

4.1 Open Loop

In the figures 9 y 10 the dynamic behaviour of the state variables is observed, validating the response of the model under the established conditions.

From the figures presented above, it is observed that the behavior of the event-driven model is reliable with respect to the operation of commercial software such as PSIM. It is noted that in open loop, voltage regulation is achieved with an overdamped behavior and a settling time of approximately 2 ms; however, it exhibits an overshoot of 50%, which makes the elements vulnerable.

Table 4: Simulation parameters

Element (Unit)	***Open Loop***	***PCMC***	***PCMC-PI***
V_{in} (V)	24	24	24
L_1, L_2 (μH)	22	22	22
R_1, R_2 (mΩ)	1.31	1.31	1.31
R (Ω)	20	20	20
C (μF)	30	30	30
f (kHz)	50	50	50
d	0.72	–	–
I_p (A)	–	30	–
V_{ref} (V)	–	–	100
k_p	–	–	0.12
k_i	–	–	1000
A	–	–	25

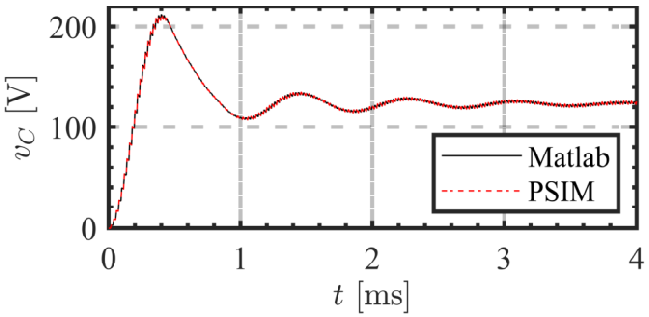

Figure 9: Open-loop voltage.

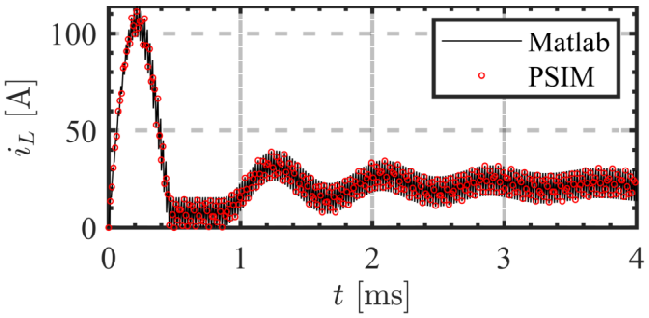

Figure 10: Open-loop current.

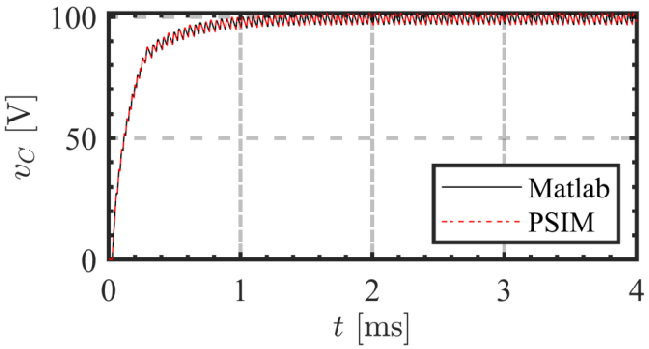

Figure 11: PCMC voltage.

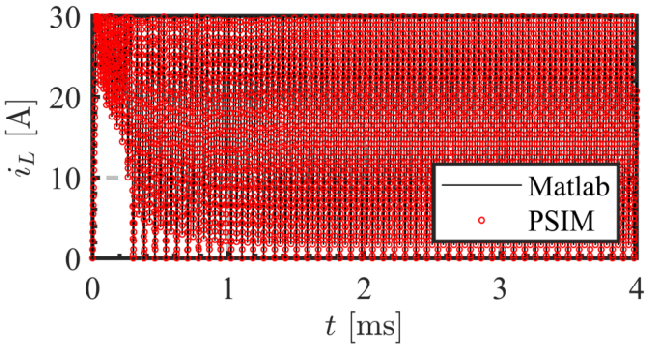

Figure 12: PCMC current.

4.2 PCMC

In the figures 11 and 12 the dynamic behaviour of the state variables is observed.

From the figures regarding the behavior of the converter controlled through PCMC, it is observed that voltage regulation is achieved while satisfying the current limiting constraint, which is beneficial for the circuit elements; however, the current exhibits a subharmonic behavior.

4.3 PCMC-PI

In the figures 13 and 14 the dynamic behaviour of the state variables is observed.

Finally, it is observed that upon implementing the PCMC-PI control, the converter achieves voltage regulation with a stable current exhibiting a periodic $1-T$ orbit. It is additionally noted

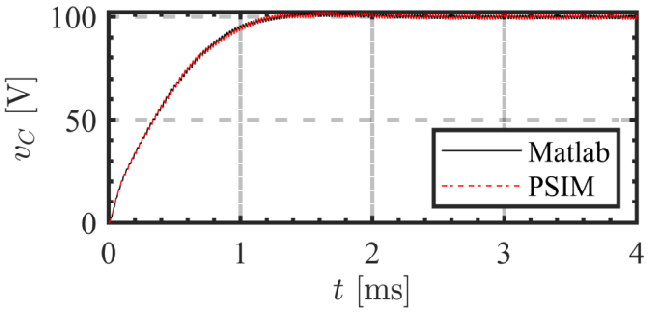

Figure 13: PCMC-PI voltage.

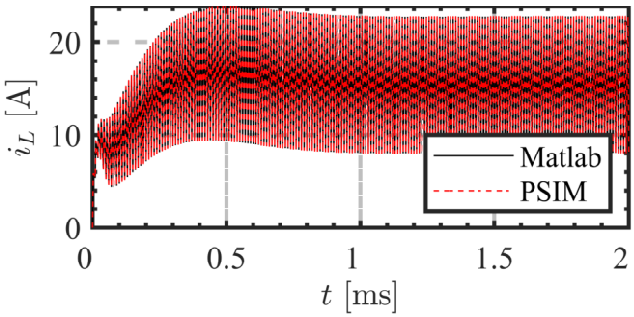

Figure 14: PCMC-PI current.

that the current flowing through the inductors is reduced, decreasing the stress imposed by this state variable on the converter elements.

5 Future Work

The event-driven model developed in this work constitutes a technical foundation oriented towards larger-scale applications in the field of renewable energy and energy storage. As a direct extension of the results obtained, it is proposed to integrate the Buck–Boost converter as the main conversion stage within a solar battery charging system. This scenario is of particular interest in regions with high irradiance, such as the Colombian Caribbean, where climatic variability and grid conditions render converter efficiency and control robustness critical performance factors [3].

To advance this proposal towards an experimental stage, it is envisaged to implement a maximum power point tracking (MPPT) algorithm directly integrated into the developed event-driven simulator, taking advantage of the model's capability to accurately detect the transition to discontinuous conduction mode through the event $i_L \leq 0$. This detection is particularly relevant under conditions of partial shading or abrupt changes in irradiance, scenarios in which conventional averaged models exhibit limitations in capturing transient dynamics. [6]. The development of a physical prototype with embedded digital control is also envisaged, in order to experimentally validate the results under real operating conditions. Furthermore, the extension of the stability analysis of the -periodic orbit through the use of jump matrices and Floquet exponents is considered, which will enable the establishment of explicit design criteria for the parameters of the PCMC-PI controller. [10].

6 Conclusions

This work has presented the modeling and event-driven simulation of a novel DC/DC Buck–Boost converter topology. The proposed configuration enables the parallel charging of the inductors and their series discharging, thereby reducing the size of the magnetic components and facilitating the extraction of a higher current from the power source. It has been demonstrated that the dynamic behavior of the converter can be fully described by three physically realizable operating topologies, whose transitions are determined by zero-crossing conditions on the state variables.

The simulation results demonstrate that the event-driven model accurately reproduces the system response in both transient and steady-state conditions, in agreement with the reference commercial software. Additionally, it is shown that the compensation ramp in the PCMC-PI

scheme extends the stability range of the converter and suppresses subharmonic behavior, thus validating this control strategy as a robust solution for applications in renewable energy and energy storage within the context of the Colombian Caribbean.

Acknowledgment

Thanks to Fundación Universitaria Antonio de Arévalo UNITECNAR and the Project "Modelado por Eventos de un Convertidor Buck-Boost con Control PI y Rampa de Compensación", also thanks to the research groups "GIRATEC: Grupo de Investigación en Robótica, Automatización, Telecomunicaciones, Electricidad, Electrónica y Computación" and "Dinámica y Control de Sistemas (DCS)" for supporting this research.

AUTHOR CONTRIBUTIONS

S.R. contributed to the conceptualization, data curation, formal analysis, funding acquisition, investigation, methodology, software, visualization and writing (original draft preparation).

H.E. contributed to the conceptualization, funding acquisition, investigation, methodology, project administration, resources, supervision, validation and writing (review & editing).

CONFLICT OF INTEREST

The authors declare that there is no conflict of interest.

RESEARCH DATA AVAILABILITY

The research data is available on demand.

AI USAGE

No artificial intelligence tools were used in this article.

References

[1] B. K. Bose, *Power Electronics in Renewable Energy Systems and Smart Grid: Technology and Applications*, ser. IEEE Press Series on Power and Energy Systems. Wiley-IEEE Press, 2019.

[2] Grand View Research, "DC-DC converter market (2024-2030)," Grand View Research, Tech. Rep., 2024. [Online]. Available: https://www.grandviewresearch.com/industry-analysis/dc-dc-converter-market-report

[3] International Renewable Energy Agency (IRENA), "Renewable power generation costs in 2023," IRENA, Tech. Rep., 2024. [Online]. Available: https://www.irena.org/Publications/2024/Sep/Renewable-Power-Generation-Costs-in-2023

[4] M. H. Rashid, *Power electronics : devices, circuits, and applications*, 4th ed. Pearson, 2014.

[5] F. Angulo, D. E. Giraldo, S. Rojas, M. A. Bolaños, G. Osorio, N. Astaiza, J. D. Mina-Casaran, and W. Herrera, "A novel nonlinear averaged model for a flyback converter with peak current mode control," in *2024 International Conference on Electrical, Computer and Energy Technologies (ICECET)*, 2024, pp. 1–6.

[6] O. Abdel-Rahim and H. Wang, "A new high gain DC-DC converter with model-predictive-control based MPPT technique for photovoltaic systems," *CPSS Transactions on Power Electronics and Applications*, vol. 5, no. 2, pp. 191–200, 2020.

[7] S. Yadav, S. Mishra, and G. Garima, "PM-BLDC motor drive for solar water pumping with modified boost converter," in *2021 8th International Conference on Signal Processing and Integrated Networks (SPIN)*, 2021, pp. 550–555.

[8] S. Rojas, D. E. Giraldo, F. Angulo, M. A. Bolaños, G. Osorio, N. Astaiza, J. Silva, and W. Herrera, "Modeling and control design of a fast capacitor charger using a power converter," in *2023 IEEE 6th Colombian Conference on Automatic Control (CCAC)*, 2023, pp. 1–5.

[9] O. Abdel-Rahim, A. Chub, A. Blinov, and D. Vinnikov, "New high-gain non-inverting buck-boost converter," in *IECON 2021–47th Annual Conference of the IEEE Industrial Electronics Society*, 2021, pp. 1–6.

[10] J. G. Muñoz Cataño, "Análisis dinámico y control de un convertidor boost-flyback," Manizales, Colombia, 2017. [Online]. Available: https://repositorio.unal.edu.co/handle/unal/63019

[11] T. Grote, F. Schafmeister, H. Figge, N. Frohleke, P. Ide, and J. Bocker, "Adaptive digital slope compensation for peak current mode control," in *2009 IEEE Energy Conversion Congress and Exposition*, 2009, pp. 3523–3529.

[12] L.-A. Ocampo, F. Angulo, G. Osorio, and D. Angulo-Garcia, "Hybrid control design of a dc/dc buck power converter," in *2019 IEEE 4th Colombian Conference on Automatic Control (CCAC)*, 2019, pp. 1–6.

[13] F. M. Bergero, "Simulación de sistemas híbridos por eventos discretos: Tiempo real y paralelismo," PhD Thesis, Universidad Nacional de Rosario, Rosario, Argentina, 2012. [Online]. Available: https://www.fceia.unr.edu.ar/~kofman/files/tesis_federico.pdf

This preprint was submitted under the following conditions:

- The authors declare that the necessary Terms of Free and Informed Consent of participants or patients in the research were obtained and are described in the manuscript, when applicable.
- The authors declare that the preparation of the manuscript followed the ethical norms of scientific communication.
- The authors declare that they are aware that they are solely responsible for the content of the preprint and that the deposit in SciELO Preprints does not mean any commitment on the part of SciELO, except its preservation and dissemination.
- The authors declare that the data, applications, and other content underlying the manuscript are referenced.
- The deposited manuscript is in PDF format.
- The authors declare that the research that originated the manuscript followed good ethical practices and that the necessary approvals from research ethics committees, when applicable, are described in the manuscript.
- The authors declare that once a manuscript is posted on the SciELO Preprints server, it can only be taken down on request to the SciELO Preprints server Editorial Secretariat, who will post a retraction notice in its place.
- The authors agree that the approved manuscript will be made available under a Creative Commons CC-BY license.
- The submitting author declares that the contributions of all authors and conflict of interest statement are included explicitly and in specific sections of the manuscript.
- The authors declare that the manuscript was not deposited and/or previously made available on another preprint server or published by a journal.
- If the manuscript is being reviewed or being prepared for publishing but not yet published by a journal, the authors declare that they have received authorization from the journal to make this deposit.
- The submitting author declares that all authors of the manuscript agree with the submission to SciELO Preprints.